Desalination and Water Treatment
www.deswater.com
doi: 10.1080/19443994.2014.921243

55 (2015) 935–944
July

Taylor & Francis
Taylor & Francis Group

Nanoporous activated carbon for fast uptake of heavy metals from aqueous solution

I. Ghiloufi[a,b,*], L. Khezami[a], L. El Mir[a,b]

[a]*College of Sciences, Al Imam Mohammad Ibn Saud Islamic University (IMSIU), Riyadh, Saudi Arabia, Tel. +96 6112582174; Fax: +96 6112586678; email: ghiloufimed@yahoo.fr (I. Ghiloufi), Tel. +96 6112581196; email: lkhezami@gmail.com (L. Khezami), Tel. +96 6112581146; email: elmirlassaad@yahoo.fr (L. El Mir)*
[b]*Laboratory of Physics of Materials and Nanomaterials Applied at Environment (LaPhyMNE), Faculty of Sciences, Gabes University, Gabes, Tunisia*

Received 27 November 2013; Accepted 29 April 2014

ABSTRACT

A novel nanoporous activated carbon (NAC), based on organic xerogel compounds, was prepared at 650°C pyrolysis temperature by sol–gel method from pyrogallol and formaldehyde (PF-650) mixtures in water using perchloric acid as catalyst. The performance of NAC was characterized by scanning electron microscopy, transmission electron microscopy, X-ray diffraction, and nitrogen porosimetry. The metal uptake characteristics were explored using well-established and effective parameters including pH, contact time, initial metal ion concentration, and temperature. Optimum adsorptions of Co^{2+} and Cd^{2+} were observed at pH 6.0 and 7.0, respectively. Langmuir model gave a better fit than the other models, and kinetic studies revealed that the adsorption is fast and its data are well fitted by the pseudo-second-order kinetic model and thermodynamic properties, i.e. ΔG°, ΔH°, and ΔS°, showed that adsorption of Co^{2+} and Cd^{2+} onto NAC was endothermic, spontaneous, and feasible in the temperature range of 300–328 K.

Keywords: Nanoporous activated carbon; Heavy metals; Adsorption; Kinetics; Thermodynamics

1. Introduction

The presence of heavy metals in industrial waste waters is particularly problematic because these metals are very soluble in the aquatic environments, and they can be absorbed by living organisms. These heavy metals enter the food chain, and accumulate in the human body on large concentrations. If they are ingested beyond the permitted concentration, they can cause serious health disorders. Therefore, it is necessary to treat metal-contaminated wastewater prior to its discharge to the environment [1].

Cadmium is a toxic heavy metal of significant environmental and occupational concern. It has been released to the environment through the combustion of fossil fuels, metal production, application of phosphate fertilizers, electroplating, and the manufacturing of batteries, pigments, and screens. This heavy metal has resulted in serious contamination of both soil and water. Cadmium (Cd) has been classified as a human carcinogen and teratogen impacting lungs, kidneys, liver, and reproductive organs [2]. Cobalt becomes

*Corresponding author.

toxic when it is not metabolized by the body and accumulates in the soft tissues. Co may enter the human body through food, water, air, or absorption through the skin when it comes in contact with humans in agriculture and in manufacturing pharmaceutical, industrial, or residential. Cobalt tends to accumulate in organisms, causing numerous diseases and disorders. It is also common groundwater contaminants at industrial and military installations [3].

There are various methods for removing heavy metals from waste water including chemical precipitation, membrane filtration, ion exchange, liquid extraction, or electrodialysis [4,5]. However, these methods are not widely used due to their high cost and low feasibility for small-scale industries [6]. In contrast, adsorption technique is by far the most versatile and widely used. Sorbents which have been studied for adsorption of metal ions include activated carbon, fly ash, crab shell, coconut shell, zeolite, manganese oxides, and rice husk. However, these adsorbents have poor removal efficiencies for low concentrations of metal ions. To prevent deteriorating surface water quality, legislation governing the levels of heavy metals, such as cadmium, lead, nickel, and zinc, discharged from industries is becoming progressively more stringent [7–10]. Thus, there is a need for exploring alternative adsorbents, with better metal removal efficiency for low aqueous concentrations.

Recently, many research groups have explored several nanoparticles for removal of heavy metals from aqueous solution, because of the ease of modifying their surface functionality and their high surface area to volume ratio for increased adsorption capacity and efficiency. For example, carbon-based nanomaterials (CNMs) are used widely in the field of removal of heavy metals in recent decades, due to its non-toxicity and high sorption capacities. Activated carbon is used firstly as sorbents, but it is difficult to remove heavy metals at ppb levels. Then, with the development of nanotechnology, carbon nanotubes, fullerene, and graphene are synthesized and used as nanosorbents of ions from wastewater, but the low sorption capacities and efficiencies limit their application deeply [11].

Pyrzyńska and Bystrzejewski [12] give the advantages and limitations of heavy metals sorption onto activated carbon, carbon nanotubes, and carbon-encapsulated magnetic nanoparticles, through sorption studies based on Co^{2+} and Cu^{2+}. The results show that carbon nanomaterials have significantly higher sorption efficiency compared to activated carbon. To enhance the sorption capacities of CNMs, they are modified by oxidation [13–15], combing with other metal ions [16] or metal oxides [17], and coupling with organic compounds [18]. Kosa et al. modified carbon nanotubes with 8-hydroxyquinoline, which are used to remove of Cu^{2+}, Pb^{2+}, Cd^{2+}, and Zn^{2+} [18].

Graphene nanosheets are synthesized through the modified Hummers method, and they are used as sorbents for the removal of Cd^{2+} and Co^{2+} ions from aqueous solution. The obtained results indicate that heavy metal ions sorption on nanosheets is dependent on pH and ionic strength, and the abundant oxygen-containing functional groups on the surfaces of graphene oxide nanosheets played an important role on sorption [19]. Chandra et al. [20] reported that magnetite–graphene adsorbents with a particle size of ~10 nm give a high binding capacity for As^{3+} and As^{5+}, and the results indicate that the high binding capacity is due to the increased adsorption sites in the graphene composite.

The aim of this work is to assess the uptake of Co^{2+} and Cd^{2+} from aqueous solution onto nanoporous activated carbon (NAC). In the first step, the synthesis by sol–gel method of NAC was reported and the effect of pyrolysis temperature on structural, morphological, and electrical properties was investigated. In second step, the efficiency of this NAC for the adsorption of the two elements from aqueous solutions was studied.

2. Material and methods

2.1. Preparation and characterization of the NAC

The preparation of NAC structure has been done in three steps. In the first one, organic xerogels were prepared by mixing formaldehyde (F) with dissolved pyrogallol (P) in water (W) solution and using picric acid as catalyst. The stoichiometric P/F and P/W molar ratios were 1/3 and 1/6, respectively. The wet gel was formed in few seconds. In the second step, the obtained product was dried in humid atmosphere at 50 °C for 2 weeks. To obtain a structured xerogel, the wet gel was transferred in an incubator and dried at 150 °C at a heating rate of 10 °C/d. The drying temperature was then maintained for 2 d. Finally in the third step, NAC structure was obtained after firing xerogel at 650 °C. In the present study, the thermal treatment was carried out in a tubular furnace under nitrogen atmosphere. The xerogel was put into a furnace and heated up to 650 °C at a heating rate of 2 °C/min to obtain NAC. The selected pyrolysis temperature was then maintained for 2 h and finally, the sample was cooled.

The synthesized product was characterized using a JEOL JSM-6300 scanning electron microscope (SEM) and a JEM-200CX transmission electron microscope (TEM). The specimens for TEM were prepared by

putting the as-grown products in ethyl alcohol and immersing them in an ultrasonic bath for 15 min, then dropping a few drops of the resulting suspension containing the synthesized materials onto TEM grid. The X-ray diffraction (XRD) patterns of NAC were carried out by a Bruker D5005 diffractometer, using Cu K radiation ($\lambda = 1.5418$ Å). The nitrogen adsorption–desorption isotherm of NAC was recorded by using Micrometrics ASAP2020 equipment.

2.2. Preparation of metal ion solution

The stock solution of cadmium and cobalt were prepared by dissolving Cadmium nitrate and cobalt nitrate in distilled water separately. The test solutions containing single cadmium and cobalt ions were prepared by diluting of 1 g/L stock metal ion solution. The initial metal ion concentration ranged from 20 to 140 mg/L. The pH of each solution was adjusted to the required value with HCl or NaOH before mixing the adsorbent. Adsorption experiments were carried in an Erlenmeyer flask by taking 10 mg of NAC in a 25 mL of metal solution at the desired temperature (25 ± 1 °C) and pH. The flasks were agitated on shaker for 12 h, which is more than ample time for adsorption equilibrium. The amount of metal adsorbed was determined by difference between the initial metal ion concentration and the final one after equilibrium was reached. The residual Cd^{2+} and Co^{2+} concentrations are measured by SPECTRO GENESIS inductively coupled plasma-atomic emission spectrometry ICP-OES.

2.3. Analysis of metal ions

The results are given as a unit of adsorbed and unadsorbed metal ion concentration per gram of adsorbent in solution at equilibrium and calculated by Eq. (1):

$$q_e = \frac{(C_0 - C_e)V}{m} \quad (1)$$

where m is the weight of adsorbent (g), q_e the adsorbed metal ion quantity per gram of adsorbent at equilibrium (mg/g), C_0 the initial metal concentration (mg/L), C_e the metal concentration at equilibrium (mg/L), and V is the working solution volume (L). The removal percentage was calculated by Eq. (2):

$$\% \text{ Removal} = \frac{(C_0 - C_e)}{C_0} \times 100 \quad (2)$$

3. Results and discussion

3.1. Adsorbent characterizations

Fig. 1 exhibits the XRD patterns of the extracted product as prepared after heat treatment at 650 °C in nitrogen atmosphere. According to this diffractogram, the samples are mostly amorphous, because of the presence of small bands centered at around 25° and 44°, corresponding to (0 0 2) and (1 0 1) hkl plans, respectively, the most intensive diffraction peaks of crystalline graphite phase.

The adsorption–desorption isotherms of the sample are of type I (Fig. 2) in the Brunauer, Emmett and Teller (BET) classification, and characteristic of microporous solid. The microporous specific surface area is 720 m^2/g determined by the conventional BET method, with micropore volume of about 0.334 cm^3/g. The mean micropore size determined from BET surface area and the pore volume in the approximation of cylindrical pores is close to 2 nm.

Fig. 3 displays the SEM micrograph of NAC sample; particles with 1–5 μm diameter appear to coagulate together leaving little space between them. The surface area and pore volume of this carbon indicate that these particles are essentially microporous. These results are consistent with porosity measurements.

TEM micrograph of NAC in Fig. 4 presents carbon nanoparticles inside microspheres. It is clearly shown that carbon microparticles consist of series of nanoparticles with diameters in the range of 10 nm. These particles are arranged in a three-dimensional network. The TEM data confirm that the interconnected solid nanoparticles comprise an open-celled network with continuous nanodimension porosity. These observations are also consistent with porosity measurements.

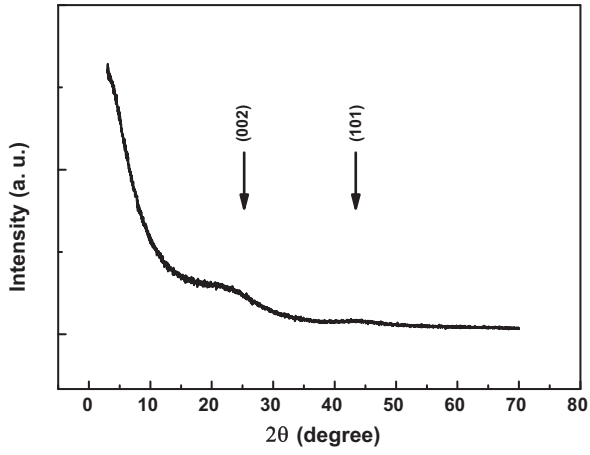

Fig. 1. XRD patterns of NAC.

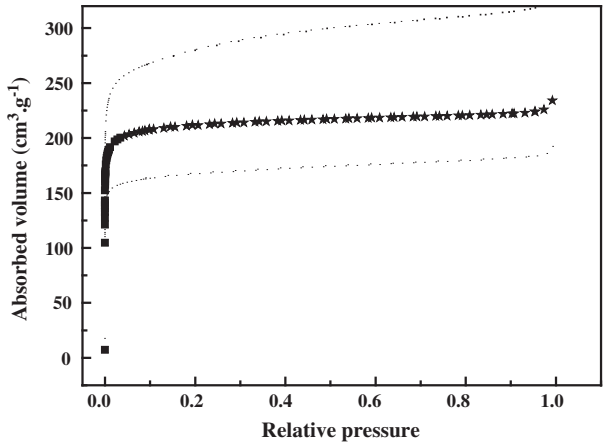

Fig. 2. Cryogenic N_2 adsorption–desorption isotherm of NAC.

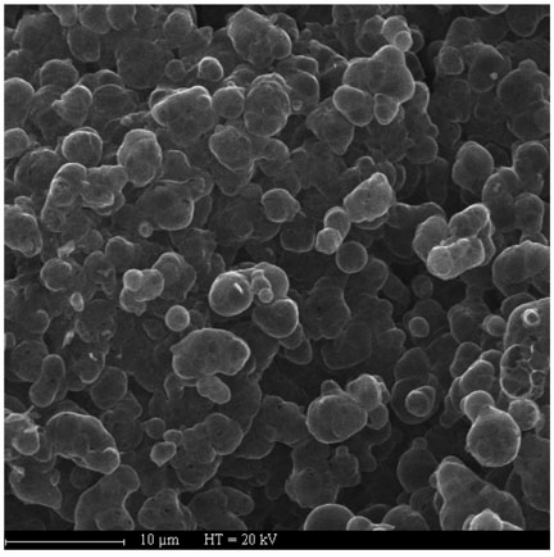

Fig. 3. SEM micrographs of NAC.

The obtained nanoporous carbon material has also a semiconductor behavior with electrical conductivity of about $4 \times 10^{-4}\,\Omega^{-1}\,cm^{-1}$ studied in our previous work [21].

3.2. Effect of pH

Earlier studies on heavy metal adsorption have shown that pH was the single most important parameter affecting the adsorption process [22]. Fig. 5 depicts the effect of initial pH on the removal of Cd^{2+} and Co^{2+} using NAC. In this study, the initial concentration of Cd^{2+} is fixed at 50 mg/L, whereas for Co^{2+} is fixed at 45 mg/L. The mass of NAC used in this study is 10 mg. This figure shows that metal

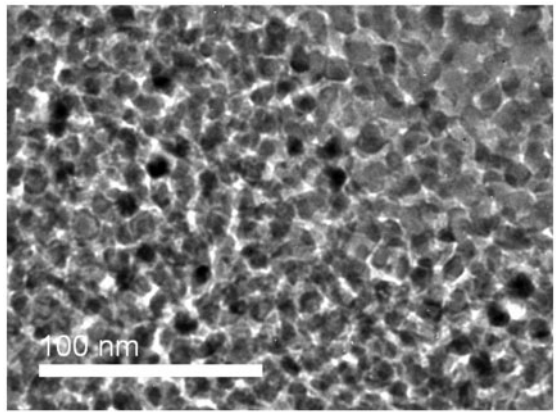

Fig. 4. TEM micrographs of ECNPC, nanoparticles inside the carbon microparticle.

adsorption by the nanoporous carbon increases with increasing pH reaching a maximum and then showed a rapid decline in adsorption. For cadmium, the sorption capacity increased significantly and reached 72.46 mg/g at pH 7, then decreased with increasing solution pH. The effect of pH on cobalt sorption shows a similar increase in sorption capacity. A sorption capacity of 41.45 mg/g was achieved at pH 6. The low metal sorption at acid solution may be explained on the basis of active sites being protonated, resulting in a competition between H^+ and M^{2+} for occupancy of the binding sites [23]. But for pH values from 6 to 10, the lower adsorption capacity of cobalt is due to precipitation. Whereas, the lower adsorption capacity of cadmium is due to lower polarity at pH 8, and precipitation for pH value more than 8.

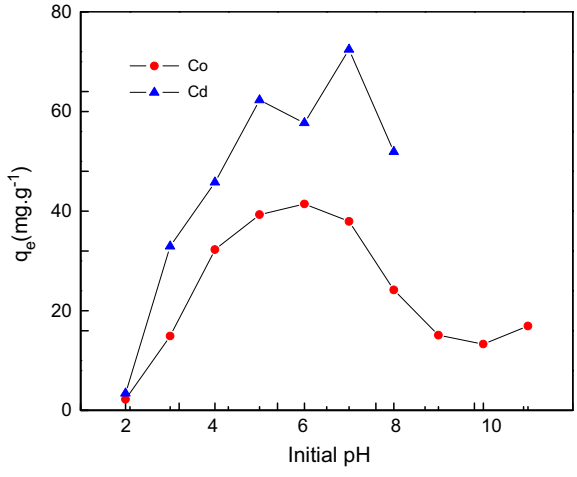

Fig. 5. Effect of initial pH on the removal of Cd^{2+} and Co^{2+} using NAC.

The effect of pH can be explained in terms of pH_{PZC} (point zero of charge) and surface site distribution of the materials [24]. The pH_{PZC} value of the adsorbent was determined to be 4.23 by the method described elsewhere [25]. AT $pH < pH_{PZC}$, the surface charge of the adsorbent is positive and the adsorption of metal (II) to the surface of adsorbent may be hindered due to the charge repulsion. At $pH > pH_{PZC}$, the surface of the adsorbent is negatively charged. Thus, the positively charged metal (II) can be easily adsorbed on the negatively charged adsorbent surface [26,27]. At lower pH, more protons may be available to protonate the active groups of adsorbent surface. This can be explained by the fact that, at low pH, the overall surface charge on the adsorbent surface became positive, which inhibited the approach of positively charged metal cations [28–30].

3.3. Effects of contact time

In this study, 100 mg of NAC is added to each 150 ml of cobalt and cadmium solutions. The initial concentrations of Cd^{2+} and Co^{2+} are fixed at 24.28 and 24.23 mg/L, respectively. Fig. 6 depicts the effect of the contact time on the sorption of Co^{2+} and Cd^{2+} by NAC. As can be seen from this figure, with the beginning of adsorption, the uptake of metal ions increased quickly, and only after 5 min, the process of adsorption reached equilibrium. After this equilibrium period, the amount of adsorbed metal ions did not significantly change with time.

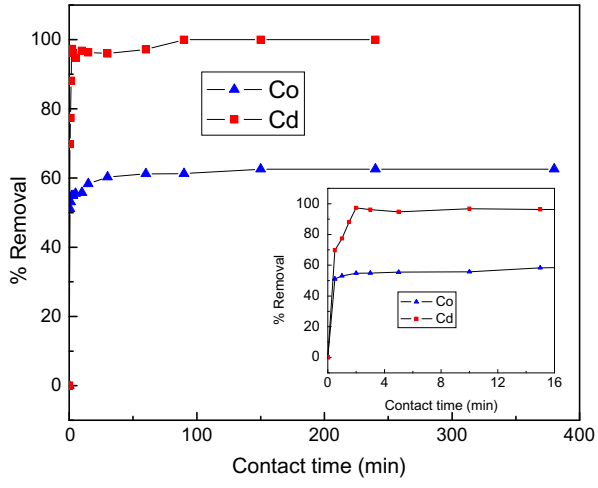

Fig. 6. Effect of contact time for Co^{2+} and Cd^{2+} removal onto NAC.

3.4. Kinetic models

The integrated linear form of the pseudo-first-order equation can be expressed as follows (Eq. (3)) [31]:

$$\ln(q_e - q_t) = \ln q_e - K_1 t \quad (3)$$

where q_e (mg g^{-1}) and q_t (mg g^{-1}) are the adsorption capacity at equilibrium and at time t (min), respectively, k_1 (min^{-1}) is the rate constant of pseudo-first-order adsorption. The straight line plots of ln ($q_e - q_t$) against t (Fig. 7) were used to determine the rate constant, k_1, q_e, and correlation coefficient R^2 values of the metal ions.

The integrated linear form of the pseudo-second-order equation can be expressed as follows (Eq. (4)) [32]:

$$\frac{t}{q_t} = \frac{1}{K_2 q_e^2} + \frac{1}{q_e} t \quad (4)$$

where k_2 (g mg^{-1} min^{-1}) is the rate constant of pseudo-second-order adsorption. The equilibrium adsorption amount (q_e) and the pseudo-second-order rate parameter (k_2) are calculated from the slope and intercept of plot of t/q_t vs. t (Fig. 8). Table 1 gives the kinetic parameters obtained from pseudo-first-order and pseudo-second-order kinetic model for Cd^{2+} and Co^{2+} adsorption on NAC.

It can be concluded from the R^2 values in Table 1 that the sorption mechanism of Cd^{2+} and Co^{2+} does not follow the pseudo-first-order kinetic model. Moreover, the experimental values of $q_{e,exp}$ are not in good agreement with the theoretical values calculated ($q_{e1,cal}$) from Eq. (3). Therefore, the pseudo-first-order

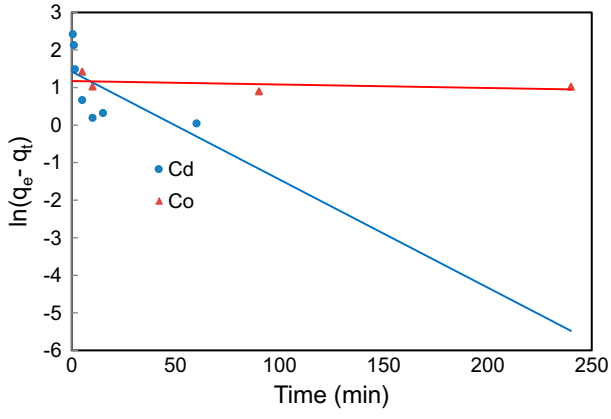

Fig. 7. Pseudo-first-order kinetic plots for Cd^{2+} and Co^{2+} adsorption onto NAC.

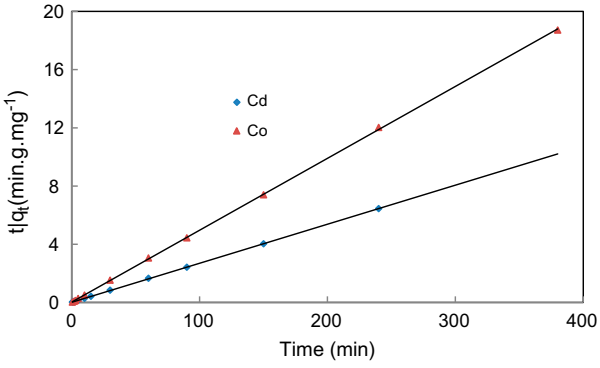

Fig. 8. Pseudo-second-order kinetic plots for Cd^{2+} and Co^{2+} adsorption onto NAC.

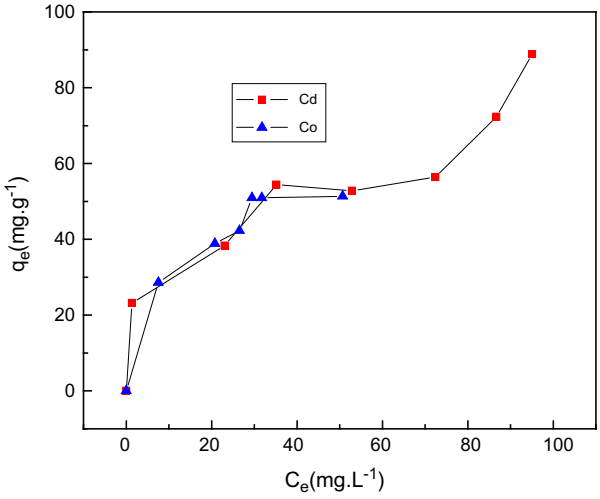

Fig. 9. Adsorption isotherm of Cd^{2+} and Co^{2+} by NAC.

model is not suitable for modeling the sorption of Cd^{2+} and Co^{2+} by NAC. However, for the pseudo-second-order, the R^2 value is 0.999 and the theoretical $q_{e2,cal}$ values were closer to the experimental $q_{e,exp}$ values (Table 1). Based on these results, it can be concluded that the pseudo-second-order kinetic model provided a good correlation for the adsorption of Cd^{2+} and Co^{2+} by NAC in contrast to the pseudo-first-order model.

3.5. Adsorption isotherms

The equilibrium adsorption isotherms are the promising data because they determine how much adsorbent is required quantitatively for enrichment of an analyte from a given solution. Cadmium and cobalt adsorption isotherms are obtained by varying the initial concentration of each metal (20–140 mg/L) at room temperature. The plot of the cadmium and cobalt adsorption capacities against their equilibrium concentration is shown in Fig. 9. For cobalt, the value of q_e increases sharply at low equilibrium concentrations, and from $C_e = 30$ mg/L the increase of q_e is slowed down and the amount of adsorbed metal ions did not significantly change. For cadmium, the variation of q_e has three steeps: in the first one, the value of q_e increases sharply at low equilibrium concentrations, in the second step when the values of C_e are between 35.15 and 72.42 mg/L, the amount of adsorbed metal ions did not significantly change, and in the last step ($C_e > 72.42$ mg/L), the value of q_e increases sharply.

Three models were used to fit the experimental data, Langmuir isotherm, Freundlich isotherm, and Temkin isotherm.

3.5.1. Langmuir isotherm

The Langmuir isotherm assumes monolayer adsorption on a uniform surface with a finite number of adsorption sites. Once a site is filled, no further sorption can take place at that site. As such, the surface will eventually reach a saturation point where the maximum adsorption of the surface will be achieved. The linear form of the Langmuir isotherm model is described as (Eq. (5)):

$$\frac{C_e}{q_e} = \frac{1}{K_m q_m} + \frac{C_e}{q_m} \quad (5)$$

where K_L is the Langmuir constant related to the energy of adsorption and q_m is the maximum adsorption capacity (mg/g) [33]. The slope and intercept of plots of

Table 1
Adsorption kinetic model rate constants for Cd^{2+} and Co^{2+} adsorption on NAC

Ion		Pseudo-first order			Pseudo-second order		
	$q_{e,exp}$ (mg/g)	k_1 (1/min)	$q_{e1,cal}$ (mg/g)	R^2	k_2 (g/mg min)	$q_{e2,cal}$ (mg/g)	R^2
Cd^{2+}	37.236	0.0287	4,138	0.397	6×10^{-2}	37.313	0.999
Co^{2+}	22.738	2×10^{-5}	3,087	0.0002	13×10^{-2}	20.242	0.999

Table 2
Langmuir, Freundlich, and Temkin, isotherm model parameters and correlation coefficients for adsorption of Cd^{2+} and Co^{2+} on NAC

Ion	Langmuir			Freundlich			Temkin		
	q_m (mg/g)	K_L (L/mg)	R^2	K_F (mg/g)	n	R^2	b_T (J/mol)	K_T (L/g)	R^2
Cd^{2+}	120.3	0.012	0.998	25.822	5.66	0.962	45.421	0.07	0.944
Co^{2+}	61.34	0.046	0.994	11.048	2.998	0.953	11.432	0.957	0.741

C_e/q_e vs. C_e were used to calculate q_m and K_L and the values of these parameters are presented in Table 2.

3.5.2. Freundlich isotherm

The Freundlich isotherm is applicable to both monolayer (chemisorption) and multilayer adsorptions (physisorption) and is based on the assumption that the adsorbate adsorbs onto the heterogeneous surface of an adsorbent [2]. The linear form of Freundlich equation is expressed as (Eq. (6)):

$$\log q_e = \log K_F + \frac{1}{n}\log C_e \quad (6)$$

where K_F (mg/g) and n are Freundlich isotherm constants related to adsorption capacity and adsorption intensity, respectively, and C_e is the equilibrium concentration (mg/L). The Freundlich isotherm constants K_F and n are determined from the intercept and slope of a plot of log q_e vs. log C_e, and they are presented in Table 2. The obtained values of n are greater than unity indicating chemisorptions [33]. Isotherms with $n>1$ are classified as L-type isotherms reflecting a high affinity between adsorbate and adsorbent and is indicative of chemisorption [33].

3.5.3. Temkin isotherm

Temkin isotherm model assumes that the adsorption energy decreases linearly with the surface coverage due to adsorbent–adsorbate interactions. The linear form of Temkin isotherm model is given by the Eq. (7):

$$q_e = b_T \ln K_T + b_T \ln C_e \quad (7)$$

where b_T is the Temkin constant related to the heat of sorption (J/mol) and K_T is the Temkin isotherm constant (L/g) [2]. K_T and b_T were determined from the intercept and slope of a plot of q_e vs. ln C_e (Table 2).

The estimated adsorption constants with corresponding correlation coefficients (R^2) are summarized in Table 2. The value of correlation coefficients obtained from each model indicates that the Langmuir model is better than the Freundlich and Temkin models to fit the experimental data, which confirms that the adsorption is a monolayer, the adsorption of each molecule has an equal activation energy, and the adsorbate–adsorbate interaction can be negligible. Thus, it is clear that the adsorption occurs on a homogeneous surface. For cadmium, the maximum adsorption capacity calculated using the Langmuir model is 120.3 mg/g at room temperature; whereas, cobalt has a maximum adsorption capacity of 61.34 mg/g.

3.6. Thermodynamic parameters

The standard Gibbs free energy ΔG° (kJ mol^{-1}) was calculated using the following Eq. (8):

$$\Delta G^\circ = -RT \ln K \quad (8)$$

Table 3
Thermodynamic parameters for adsorption of heavy metals on NAC

Ion	T (K)	k	ΔG° (kJ mol^{-1})	ΔS° (kJ mol^{-1} K^{-1})	ΔH° (kJ mol^{-1})
Cd^{2+}	300	3.7648	−3.307	55.3487	13.382
	313	4.264	−3.774		
	328	5.9413	−4.860		
Co^{2+}	300	1.8202	−1.494	42.722	11.197
	313	2.5464	−2.433		
	328	2.6773	−2.686		

where K is the thermodynamic equilibrium constant, or the thermodynamic distribution coefficient, and it can be defined as (Eq. (9)):

$$K = \frac{a_s}{a_e} = \frac{\gamma_s C_s}{\gamma_e C_e} \quad (9)$$

where a_e is the activity of metal ion in solution at equilibrium; a_s is the activity of adsorbed metal ion; C_s is the surface concentration of metal ion (mmol g^{-1}) in the adsorbent; C_e is the metal ion concentration in solution at equilibrium (mmol mL^{-1}); γ_e represent the activity coefficient of the metal ion in solution; and γ_s is the activity coefficient of the adsorbed metal ion. As the metal ion concentration in the solution declines to zero, k can be obtained by plotting ln (C_s/C_e) vs. C_s and extrapolating C_s to zero [34,35]. The straight line obtained fitted the points by least-squares analysis. The intercept at the vertical axis yields the values of k. The obtained values of k and ΔG^o at different temperatures are given in Table 3.

The average standard enthalpy change (ΔH^o) and entropy change (ΔS^o) of metal ion adsorption onto NAC were calculated by the following Eq. (10):

$$\ln K = \frac{\Delta S^\circ}{R} - \frac{\Delta H^\circ}{RT} \quad (10)$$

where ΔH^o and ΔS^o were calculated from the slope and the intercept, respectively, in the plot of ln (k) against 1/T [36]. These results are shown in Fig. 10. Table 3 presents the obtained values of ΔH^o and ΔS^o at different temperature for metal ion adsorption process on NAC.

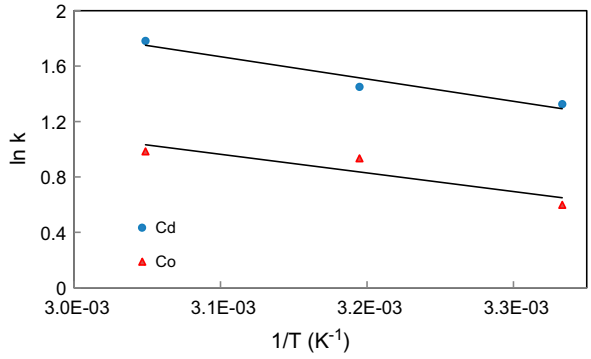

Fig. 10. Plot of ln k vs. 1/T for the estimation of thermodynamic parameters for adsorption of Cd^{2+} and Co^{2+} on NAC.

The thermodynamic equilibrium constant k increased with temperature indicating that the adsorption was endothermic. Negative values of ΔG^o for the two metal ions indicate spontaneous adsorption and the degree of spontaneity of the reaction increases with increasing temperature. The values of standard enthalpy change for Cd^{2+} and Co^{2+} are positive, this suggests that the adsorption of Cd^{2+} and Co^{2+} by NAC is endothermic, which is supported by the increasing of adsorption with temperature for the two elements. The positive standard entropy change of Cd^{2+} and Co^{2+} reflects the affinity of the NAC towards the two metal ions [33].

Table 4
Comparison of adsorption capacities of various adsorbents for Co^{2+} and Cd^{2+}

Adsorbent	q_e (mg g^{-1})	Temp. (K)	pH	Ref.
Cd^{2+}				
Ag-MWCNTs	54.92	313	7.0	[24]
AC (Cicer arietinum)	18	273	8.0	[37]
CNTs (MnO_2 coated)	9.1	273	6.0	[38]
CNT (HNO_3)	11.0	–	–	[39]
MWCNT (HNO_3)	10.86	–	–	[40]
MWCNT (HNO_3)	31.0	–	–	[41]
nZVI	769.2	297		[33]
NAC	120.3	300	6.5	This work
Co^{2+}				
HApZ	10.892	303	6	[42]
Peat moss	29.75	292.5	6	[43]
F 300 D carbon	6.24	298	–	[44]
Natural bentonite	15.2	–	6	[45]
CEMNP	3.21 mg/g	–	8	[12]
CNTs	2.77 mg/g	–	8	[12]
NAC	61.34	300	6.5	This work

3.7. Comparison of Cd and Co adsorption capacity among different adsorbents

The adsorption capacity of NAC for the removal of Cd^{2+} and Co^{2+} has been compared with various adsorbents reported in literatures and their adsorption capacities are summarized in Table 4. A comparison between our work and the reported data from the literature [2,12,24,37–45] shows that NAC is more efficient and promising adsorbent for Co^{2+} and Cd^{2+} removal than other nanostructure adsorbents. Therefore, it can be safely concluded that the NAC have a considerable potential for the removal of Co^{2+} and Cd^{2+} from water and wastewater.

4. Conclusion

The adsorbent NAC was identified as potential and highly efficient nanoporous structure for the fast removal of Co^{2+} and Cd^{2+} from water, the adsorption depends strongly on different parameters like pH and temperature. Kinetic studies revealed that the equilibrium was reached within 5 min and the pseudo-second-order kinetic model provides the best correlation with the experimental data compared to the pseudo-first-order model. The maximum adsorption capacity of Cd^{2+} and Co^{2+} was found to be 120.3 and 61.34 mg g^{-1}, respectively, under pH of 6.5, and temperature of 300 K. The Langmuir model yields a better fitting than the Freundlich and Temkin models for metal ion adsorption on NAC under the investigated temperatures, hence the adsorption is monolayer. From the thermodynamic studies, the adsorption process was spontaneous and endothermic. These results provide the enhancement of the Co^{2+} and Cd^{2+} uptake from aqueous solutions by NAC which are considered as adsorbents for removing the metals from water and waste water.

Acknowledgments

This work was supported by the National Plan, for Sciences, Technology and innovation, at Al-Imam Mohammed Ibn Saud Islamic University, college of Sciences, Kingdom of Saudi Arabia.

References

[1] S. Babel, T.A. Kurniawan, Cr(VI) removal from synthetic wastewater using coconut shell charcoal and commercial activated carbon modified with oxidizing agents and/or chitosan, Chemosphere 54(7) (2004) 951–967.
[2] K.H. Boparai, M. Joseph, D.M. O'Carroll, Kinetics and thermodynamics of cadmium ion removal by adsorption onto nano zerovalent iron particles, J. Hazard. Mater. 186 (2011) 458–465.
[3] S.A. Abo-Farha, A.Y. Abdel-Aal, I.A. Ashour, S.E. Garamon, Removal of some heavy metal cations by synthetic resin purolite C100, J. Hazard. Mater. 169 (2009) 190–194.
[4] M. Sitting, Handbook of Toxic and Hazardous Chemicals, Noyes Publications, Park Ridge, NJ, 1981.
[5] J.W. Patterson, Industrial Wastewater Treatment Technology, 2nd ed., Butterworth-Heinemann, London, 1985.
[6] A. Sohail, S.I. Ali, N.A. Khan, R.A.K. Rao, Removal of chromium from wastewater by adsorption, Environt. Pollut. Control 2 (1999) 27–31.
[7] T.A. Kurniawan, G.Y.S. Chan, W. Lo, S. Babel, Comparisons of low-cost adsorbents for treating wastewaters laden with heavy metals, Sci. Total Environ. 366 (2–3) (2006) 409–426.
[8] S. Babel, T.A. Kurniawan, Low-cost adsorbents for heavy metals uptake from contaminated water: A review, J. Hazard. Mater. 97(1–3) (2003) 219–243.
[9] S.E. Bailey, T.J. Olin, R.M. Bricka, D.D. Adrian, A review of potentially low-cost sorbents for heavy metals, Water Res. 33(11) (1999) 2469–2479.
[10] V.C. Srivastava, I.D. Mall, I.M. Mishra, Adsorption thermodynamics and isosteric heat of adsorption of toxic metal ions onto bagasse fly ash (BFA) and rice husk ash (RHA), Chem. Eng. J. 132(1–3) (2007) 267–278.
[11] M.S. Mauter, M. Elimelech, Environmental applications of carbon-based nanomaterials, Environ. Sci. Technol. 42 (2008) 5843–5859.
[12] K. Pyrzyńska, M. Bystrzejewski, Comparative study of heavy metal ions sorption onto activated carbon, carbon nanotubes, and carbon-encapsulated magnetic nanoparticles, Colloids Surf. A 362 (2010) 102–109.
[13] A. Stafiej, K. Pyrzynska, Adsorption of heavy metal ions with carbon nanotubes, Sep. Purif. Technol. 58 (2007) 49–52.
[14] G.P. Rao, C. Lu, F. Su, Sorption of divalent metal ions from aqueous solution by carbon nanotubes: A review, Sep. Purif. Technol. 58 (2007) 224–231.
[15] D. Afzali, R. Jamshidi, S. Ghaseminezhad, Z. Afzali, Preconcentration procedure trace amounts of palladium using modified multiwalled carbon nanotubes sorbent prior to flame atomic absorption spectrometry, Arab. Chem. 5(4) (2012) 461–466.
[16] V.K. Gupta, S. Agarwal, T.A. Saleh, Synthesis and characterization of alumina coated carbon nanotubes and their application for lead removal, J. Hazard. Mater. 185 (2011) 17–23.
[17] X. Zhao, Q. Jia, N. Song, W. Zhou, Y. Li, Adsorption of Pb(II) from an aqueous solution by titanium dioxide/carbon nanotube nanocomposites: Kinetics, thermodynamics, and Isotherms, J. Chem. Eng. Data 55 (2010) 4428–4433.
[18] S.A. Kosa, G. Al-Zhrani, M. Abdel Salam, Removal of heavy metals from aqueous solutions by multi-walled carbon nanotubes modified with 8-hydroxyquinoline, Chem. Eng. J. 181–182 (2012) 159–168.
[19] L.K. Wang, D.A. Vaccari, Y. Li, N.K. Shammas, Chemical precipitation, in: L.K. Wang, Y.T. Hung, N.K. Shammas (Eds.), Physicochemical Treatment

Processes, vol. 3, Humana Press, New Jersey, 2004, pp. 141–198.
[20] V. Chandra, J. Park, Y. Chun, J.W. Lee, I.C. Hwang, Water-dispersible magnetite-reduced graphene oxide composites for arsenic removal, ACS Nano 4 (2010) 3979–3986.
[21] N. Ben Mansour, I. Najeh, H. Dahman, L. El Mir, Effect of nickel concentration on electrical properties of carbon–nickel nanocomposite, Sensor Lett. 9 (2011) 2171–2174.
[22] Y. Prasanna Kumar, P. King, V.S.R.K. Prasad, Comparison for adsorption modelling of copper and zinc from aqueous solution by Ulva fasciata sp, J. Hazard. Mater. 137 (2006) 1246–1251.
[23] J.M. Tobin, D.G. Cooper, R.J. Neufeld, Uptake of metal ions by Rhizopus arrhizus biomass, Appl. Environ. Microb. 47 (1984) 821–824.
[24] D.K. Venkata Ramana, J.S. Yu, K. Seshaiah, Silver nanoparticles deposited multiwalled carbon nanotubes for removal of Cu(II) and Cd(II) from water: Surface, kinetic, equilibrium, and thermal adsorption properties, Chem. Eng. J. 223 (2013) 806–815.
[25] R. Leyva-Ramos, L.A. Bernal-Jacome, I. Acosta-Rodriguez, Adsorption of cadmium(II) from aqueous solution on natural and oxidized corncob, Sep. Purif. Technol. 45 (2005) 41–49.
[26] D.D. Shao, Z.Q. Jiang, X.K. Wang, SDBS modified XC-72 carbon for the removal of Pb(II) from aqueous solutions, Plasma Processes Polym. 7 (2010) 552–560.
[27] M.A. Adolph, Y.M. Xavier, P. Kriveshini, K. Rui, Phosphine functionalized multiwalled carbon nanotubes: A new adsorbent for the removal of nickel from aqueous solution, J. Environ. Sci. 24(6) (2012) 1133–1141.
[28] F. Luo, Y. Liu, X. Li, Z. Xuan, J. Ma, Biosorption of lead ion by chemically modified-biomass of marine brown algae Laminaria japonica, Chemosphere 64 (2006) 1122–1127.
[29] J.L. Zhou, P.L. Huang, R.G. Lin, Sorption and desorption of Cu and Cd by macroalgae and microalgae, Environ. Pollut. 101 (1998) 67–75.
[30] N.C.M. Gomes, V.R. Linardi, Removal of gold, silver and copper by living and nonliving fungi from leach liquor obtained from the gold mining industry, Rev. Microbiol. 27 (1996) 218–222.
[31] S. Lagergren, Zur theorie der sogenannten adsorption geloster stoffe kungliga svenska vetenskapsakademiens [For the theory of so-called adsorption of dissolved substances], Handlingar 24 (1898) 1–39.
[32] Y.S. Ho, G. McKay, D.A.J. Wase, C.F. Forster, Study of the sorption of divalent metal ions on to peat, Adsorpt. Sci. Technol. 18 (2000) 639–650.
[33] C.H. Yang, Statistical mechanical study on the Freundlich isotherm equation, J. Colloid Interface Sci. 208 (1998) 379–387.
[34] N. Chiron, R. Guilet, E. Deydier, Adsorption of Cu(II) and Pb(II) onto a grafted silica: Isotherms and kinetic models, Water Res. 37 (2003) 3079–3086.
[35] Y.-J. Tu, C.-F. You, C.-K. Chang, Kinetics and thermodynamics of adsorption for Cd on green manufactured nano-particles, J. Hazard. Mater. 235–236 (2012) 116–122.
[36] Z. Aksu, Determination of the equilibrium, kinetic and thermodynamic parameters of the batch biosorption of nickel(II) ions onto chlorella vulgaris, Process Biochem. 38 (2002) 89–99.
[37] D.K.V. Ramana, K. Jamuna, B. Satyanarayana, B. Venkateswarlu, M. Rao, Removal of heavy metals from aqueous solutions using activated carbon prepared from Cicer arietinum, Toxicol. Environ. Chem. 92(8) (2010) 1447–1460.
[38] B.W. Yang, Q. Gong, L. Zhao, H. Sun, N. Ren, J. Qin, J. Xu, H. Yang, Preconcentration and determination of lead and cadmium in water samples with a MnO_2 coated carbon nanotubes by using ETAAS, Desalination 278 (2011) 65–69.
[39] Y.H. Li, S. Wang, Z. Luan, J. Ding, C. Xu, D. Wu, Adsorption of cadmium (II) from aqueous solution by surface oxidized carbon nanotubes, Carbon 41 (2003) 1057–1062.
[40] Y.H. Li, J. Ding, Z. Luan, Z. Di, Y. Zhu, C. Xu, D. Wu, B. Wei, Competitive adsorption of Pb(II), Cu(II) and Cd(II) ions from aqueous solutions by multiwalled carbon nanotubes, Carbon 41 (2003) 2787–2792.
[41] P. Liang, Y. Liu, L. Guo, J. Zeng, H. Lu, Multiwalled carbon nanotubes as solid phase extraction adsorbent for the preconcentration of trace metal ions and their determination by inductively coupled plasma atomic emission spectrometry, J. Anal. At. Spectrom. 19 (2004) 1489–1492.
[42] N. Gupta, A.K. Kushwaha, M.C. Chattopadhyaya, Adsorption of cobalt(II) from aqueous solution onto hydroxyapatite/zeolite composite, Adv. Mater. Lett. 2 (4) (2011) 309–312.
[43] C. Caramalău, L. Bulgariu, M. Macoveanu, Cobalt (II) removal from aqueous solutions by adsorption on modified peat moss, Chem. Bull. 54(68) (2009) 13–17 "POLITEHNICA" Univ. (Timisoara).
[44] Y.V. Hete, S.B. Gholase, R.U. Khope, Adsorption study of cobalt on treated granular activated carbon, J. Chem. 9(1) (2012) 335–339.
[45] F. Ghomri, A. Lahsini, A. Laajeb, A. Addaou, The removal of heavy metal ions (copper, zinc, nickel and cobalt) by natural bentonite, Int. Rev. Chem. Eng. 4(4) (2012) 37–54.